diffusion-fundamentals

The Open-Access Journal for the Basic Principles of Diffusion Theory, Experiment and Application

Applications of Pulsed Gradient Spin-Echo NMR Diffusion Measurements to Solution Dynamics and Organization

William S. Price

Nanoscale Organization and Dynamics Group
College of Science, Technology and Environment
University of Western Sydney, Penrith South, NSW 1797, Australia

Corresponding author:
Prof. William S. Price
Nanoscale Organization and Dynamics Group
College of Science, Technology and Environment
University of Western Sydney, Penrith South,
NSW 1797,
Australia
Ph: (+61 2) 4620 3336
Fax: (+61 2) 4620 3025
e-mail: w.price@uws.edu.au

Abstract

The study of solution dynamics is a very fundamental area of research with wide ranging importance from physical chemistry through to the life sciences. A common theme is that the interactions which control the dynamics and organization of solutions are generally very weak. Translational diffusion provides a non-invasive, direct and natural probe of the dynamics and pulsed gradient spin-echo (PGSE) NMR is a convenient means of measuring diffusion. This paper gives a brief introduction to translational diffusion as a probe of solution dynamics and of the PGSE NMR method before presenting some representative examples illustrating the power of diffusion measurements for elucidating the molecular behaviour. The use of PGSE NMR to study solution dynamics and organization is a very active area of research and a very large literature already exists, consequently, the coverage of possible applications and the literature cited here is not comprehensive.

Key Words: Association, Binding, Diffusion, DOSY, NMR, PGSE NMR.

1. Solution Dynamics and Organization

Despite the simple attractiveness of the idea, solutions are rarely perfectly homogeneous. Indeed, even if a solution can be described as homogeneous it is probably only true over a limited temperature range or length scale. An obvious example would be water, which has very complicated solution dynamics by virtue of its intricate hydrogen bonding network. In the bulk liquid state and over a sufficiently long time-scale the dynamics of the water molecules is likely to appear highly random. At a shorter length scale and at shorter time-scale some degree of ordering is certainly apparent. As the temperature is reduced the dynamics change and at some point the organization in the solution becomes highly ordered and the phase we know as ice appears [1]. As a second example, at a length scale greater than nanometres the ordering of water molecules in a lithium chloride solution appears random. In reality, many of the water molecules are at least transiently confined to hydration layers around the lithium ion [2].

The non-purely homogenous nature and non-random dynamics of molecules confer extremely important and 'non-ideal' properties on solutions. In fact, such small scale solution organization is the link to large scale structures such as the formation of lipid bilayers which make biological systems possible.

A common theme in solution organization is that the solutions are fragile systems. Consequently, any reliable method for probing them must be effectively non-invasive. An ideal handle for studying solution structure would be one that afforded information not only on the particular solution species under study, but on the local environment. Translational diffusion (not to be confused with mutual diffusion) provides just such a handle because changes in size and the surrounding environment directly affect it. NMR provides a non-invasive and convenient means of probing this and the method is known as the pulsed gradient spin-echo (PGSE) method and throughout the literature it is also commonly referred to as affinity NMR, DOSY, PFG NMR or NMR diffusometry. The method is extremely powerful and extraordinarily applicable to studying solution properties as is evident from the large and rapidly growing literature. Under favourable conditions and with the best of contemporary equipment, the PGSE method is capable of measuring diffusion down to about 10^{-14} m^2s^{-1}. Numerous reviews of a general nature have appeared [3-10] as well as those concentrating on specific areas of solution chemistry including polymer gels [11], proteins [12], surfactants [13,14], and binding and exchange [15-18].

2. Diffusion, Viscosity and Hydrodynamics

In this section a short introduction to diffusion is given and why it provides such a powerful probe of solution structure and organization. Diffusion is the (stochastic) random thermal motion of a species (e.g., molecule or ion) and is the most fundamental form of transport [19-21]. At very short time-scales diffusion is a many-body problem, but at sufficiently large times it reduces to a single-body stochastic problem characterized by a single number, the self-diffusion coefficient D, viz. (see [22])

$$D = \lim_{t\to\infty} \frac{1}{6t} \left\langle \left| \mathbf{r}_i(t) - \mathbf{r}_i(0) \right|^2 \right\rangle \quad (1)$$

where $\mathbf{r}_i(t)$ is the location of particle i at time t and the angled brackets denote the ensemble average. In a rapidly diffusing liquid such as water, the concept of a diffusion coefficient holds for times longer than 10 ps [23]. At times shorter than this (in viscous systems this time would be longer than 10 ps) 'anomalous' diffusion may be observed. Under ideal conditions, the diffusion coefficient of a species can be correlated with the available thermal energy (i.e., kT where k is the Boltzmann constant and T is temperature) by way of the Stokes-Einstein equation [24,25],

$$D = \frac{kT}{f} \quad (2)$$

where f is the friction coefficient. For the simple case of a spherical particle with a Stokes radius (i.e., the effective hydrodynamic radius) r_S (m) in a solvent of viscosity η (Pa s = 10 Poise) the friction factor is given by

$$f = b\pi\eta r_S . \quad (3)$$

The dimensionless parameter b reflects the boundary conditions between the solvent and the moving particle and (normally) ranges between 4 (the so called slip condition) to 6 (the stick condition). From the Stokes Einstein equation it can be seen that $D \propto Mw^{-1/3}$ (with Mw = molecular weight).

The Stokes-Einstein equation is valid only under ideal conditions in which diffusing species sees the solvent as a continuum and that the diffusing species are essentially at infinite dilution (allowing interactions between diffusing species to be ignored). Despite its serious limitations, the Stokes-Einstein equation provides a useful and intuitive framework for the interpretation of diffusion data.

3. NMR Diffusion Measurements

The mechanism underlying PGSE NMR diffusion measurements is surprisingly simple: Coherent transverse nuclear magnetization is transformed ('encoded') into a well-defined spatial structure, a helix, which is then corrupted by translational diffusion during a precise duration, Δ. The process that formed the helix is then reversed, but due to the corruption of the helix the unencoding of the coherent transverse magnetization is imperfect. The recovered transverse magnetization is then measured. The greater the diffusion during Δ, the less successful the restoration and thus, the smaller the resulting NMR signal. The devil lies in the technical details for encoding and decoding the magnetization and the theory relating the loss in NMR signal to the diffusive processes.

Spatial encoding and decoding

The spatial encoding and decoding of the magnetization in diffusion experiments is normally performed as part of a modified spin-echo pulse sequence (normally a Hahn-

echo [26] or stimulated-echo [27]). Using the Hahn spin-echo as an example, magnetization which is initially oriented along the z-axis is converted to transverse magnetization by a (typically) $\pi/2$ rf pulse. This magnetization is then subject to a pulse of a constant magnetic field gradient which winds the magnetization into a helix along the direction of the gradient. This occurs since, during the gradient pulse, the Larmor precession frequency will change with position, and taking the gradient to be directed along the z-direction (i.e., g_z), we have

$$\omega(z) = \gamma B_0 + \gamma g_z z \tag{4}$$

where γ is the gyromagnetic ratio and the first term represents the contribution from the static field (B_0) and, excluding the effects of imperfections and sample inhomogeneity with respect to magnetic susceptibility [28], it is the same for all spins in the sample. It is the second term, which is due to the applied gradient, that is of primary interest as it is this term which provides the spatial dependence to the Larmor frequency and thereby the mechanism for winding the magnetization into a helix. A magnetic gradient pulse of length δ and magnitude and direction $\mathbf{g}$ (i.e., 'area' = $\delta\mathbf{g}$) leads to the definition of the reciprocal space vector

$$\mathbf{q} = (2\pi)^{-1} \gamma \mathbf{g} \delta \quad (\mathrm{m}^{-1}). \tag{5}$$

The application of an infinitely short gradient pulse (i.e., $\delta \to 0$ and $|\mathbf{g}| \to \infty$ while δg remains finite) with $\mathbf{g}$ directed along the long axis of a cylindrical sample would transform the transverse magnetization into a helix with pitch q^{-1} (m). As it is diffusion that is of interest and not the effects of chemical shift evolution, a π rf pulse is applied at the point τ during the sequence. Since the π pulse reverses the sign of the phase change that has accumulated prior to its application, an identical unencoding gradient pulse is applied at a time Δ later as schematically represented in **Figure 1**. The key point is that z in Eq. (4) is time-dependent (i.e., $z(t)$) due to diffusion and thus the phase change acquired during the first τ period will not be counteracted by that acquired in the second τ period.

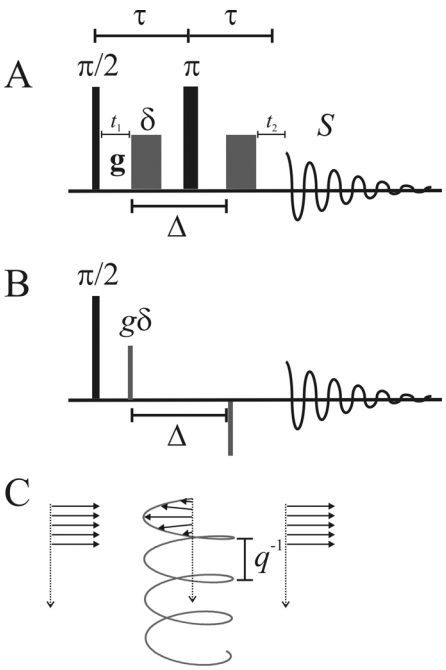

Figure 1 (A) A Hahn spin-echo based PGSE sequence in which two equal gradient pulses of duration δ and direction and magnitude g are inserted into each τ period. δ is typically in the range of 1 – 10 ms, and the separation Δ between the leading edges of the gradient pulses is normally in the range of 10 ms to 1 s. The second half of the echo is used as the NMR signal (S. i.e., the FID). It is convenient to define the echo attenuation as the ratio of the echo signal S(g) to that signal with no applied gradient S(0), viz. $E(g) = S(g)/S(g=0)$, as it allows the effects of spin-spin relaxation to be normalized out. (B) In the short gradient pulse approximation the gradient pulses are assumed to be infinitely short but $g\delta$ is finite. (C) An example of the encoding of coherent magnetization into a helix (the arrows represent nuclear spins and the spiral curve is a guide for the eye), that would be formed by applying a gradient pulse along the long axis of a cylindrical sample. In the absence of diffusion, a second identical but effectively negative gradient pulse would completely refocus the magnetization.

Technically the experiment is difficult, as the applied gradient must be constant throughout the sample and ideally the gradient pulses are kept as short as possible as this allows the effects of diffusion during the gradient pulses to be ignored. Additional complications arise from eddy currents that are generated from the rapidly changing gradients, gradient mismatch [29], convection [30,31], and radiation damping [32].

Relating the PGSE NMR signal to the underlying diffusion processes

Various means exist for relating the PGSE attenuation to the underlying diffusion processes (see [33] for a brief discussion). The most conceptually straightforward approach is that of the short gradient pulse approximation (SGP) [34]. This approximation makes the assumption that motion during the gradient pulse can be neglected such that the helix formation is not corrupted during the pulse, and leads to the SGP relation for the spin-echo attenuation [34]

$$E(\mathbf{q}) = \int\int \rho(\mathbf{r}_0)\, P(\mathbf{r}_0, \mathbf{r}_1, \Delta)\; \mathrm{e}^{i2\pi\mathbf{q}\cdot(\mathbf{r}_1-\mathbf{r}_0)}\, \mathrm{d}\mathbf{r}_0\; \mathrm{d}\mathbf{r}_1 \tag{6}$$

where $\rho(\mathbf{r_0})$ is the equilibrium spin-density and $P(\mathbf{r}_0, \mathbf{r}_1, \Delta)$ is the diffusion propagator [35] (or Green function [36]) derived using appropriate boundary conditions and a delta function initial condition. The integral is taken over all starting ($\mathbf{r}_0$) and finishing ($\mathbf{r}_1$) positions. Eq. (6) states that the echo attenuation is given by the Fourier transform of the diffusion propagator with respect to **q**. In the case of free isotropic diffusion, Eq. (6) leads to the simple single-exponential relation,

$$E = \exp\left(-4\pi^2 q^2 D\Delta\right). \tag{7}$$

Often though, it is not technically possible to make pulses short enough so that motion can be neglected during the gradient pulses. Starting from the Bloch-Torrey equations [37] the analytically correct solution is given by [26,38]

$$E = \exp\left(-4\pi^2 q^2 D\left(\Delta - \delta/3\right)\right). \tag{8}$$

The δ/3 term in Eq. (8) corrects for the motion during the gradient pulse. Unfortunately, such a simple correction for the effects of the finite duration of gradient pulses does not apply to more complicated translational motions [33].

4. Exchange

Any form of molecular association can theoretically be studied using a PGSE measurement since the association will change the size and shape of the diffusing species. If the binding process is reversible and occurs on a time-scale similar to that of the diffusion measurement (i.e., Δ) additional information regarding the dynamics of the exchange process may also become evident. Consider the case of a simple two-site system as depicted in **Figure 2**, in which a low molecular weight species such as a ligand (L) exchanges between being located in free solution to any one of *n* equivalent binding sites on a high molecular weight species such as a protein (P) with a dissociation constant K_d (i.e., $\mathrm{PL} \overset{K_\mathrm{d}}{\leftrightarrow} \mathrm{P+L}$).

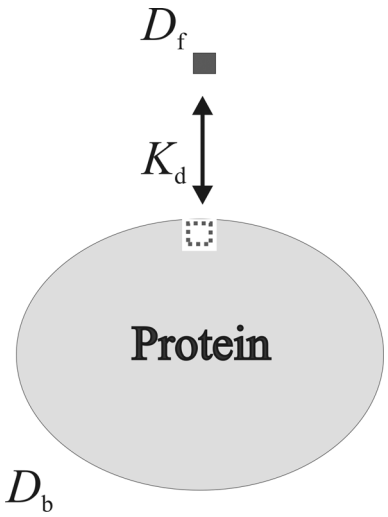

Figure 2. A schematic diagram of a two-site binding model of a ligand (square) with a free diffusion coefficient of D_f, in exchange with a binding site on a protein. The diffusion coefficient of the bound ligand is D_b, and is taken as being equal to that of the protein.

The theory relating the spin echo attenuation to the dynamics of an exchanging two-site system has been presented by Kärger and co-workers (e.g., see ref. [5]). The model is implemented in the short gradient pulse limit and it is assumed that the exchanging species undergoes free diffusion in both sites. The coupled differential equations describing the echo signal intensities at the free and bound sites are,

$$\begin{aligned} \frac{dS_f}{dt} &= -\gamma^2 g^2 D_f \delta^2 S_f - \frac{S_f}{\tau_f} + \frac{S_b}{\tau_b} \\ \frac{dS_b}{dt} &= -\gamma^2 g^2 D_b \delta^2 S_b - \frac{S_b}{\tau_b} + \frac{S_f}{\tau_f} \end{aligned} \tag{9}$$

where τ_f and τ_b are the lifetimes in the free and bound sites, respectively. The initial conditions are given by $S_f\big|_{t=0} = P_f = (1 - P_b)$ and $S_b\big|_{t=0} = P_b$ where P_f and P_b are the populations in the free and bound sites, respectively.

The solution to these equations is given by,

$$E(q,\Delta) = C_A e^{-q^2 D_A \Delta} + C_B e^{-q^2 D_B \Delta} \tag{10}$$

where D_A and D_B are the apparent self-diffusion coefficients defined below and C_A and C_B are the population fractions (relative signal intensities)

$$D_{A,B} = \frac{1}{2}\left\{ D_b + D_f + \frac{1}{q^2}\left(\frac{1}{\tau_b} + \frac{1}{\tau_f}\right) \pm \sqrt{\left[D_b - D_f + \frac{1}{q^2}\left(\frac{1}{\tau_b} - \frac{1}{\tau_f}\right)\right]^2 + \frac{4}{q^4 \tau_b \tau_f}} \right\} \quad (11)$$

$$C_A = 1 - C_B \quad (12)$$

and

$$C_B = \frac{P_b D_b + P_f D_f - D_A}{D_B - D_A} \quad (13)$$

and D_b and D_f are the diffusion coefficients of the bound and free ligand, respectively. Similarly P_b and P_f are the relative populations and τ_b and τ_f (not to be confused with the τ delay in the PGSE sequence) are the mean residence lifetimes at each site. Thus, the effect of diffusion on the signal intensity when transport occurs between two, freely diffusing, sites (ignoring relaxation time differences between the two sites) is given by a superposition of exponentials [5].

At $t = \Delta$ and in the case of fast exchange, this reduces to the particularly simple single exponential form,

$$E = S_b + S_f = \exp\left(-\gamma^2 g^2 D_{obs} \delta^2 \Delta\right) \quad (14)$$

where

$$D_{obs} = \left(1 - P_b\right) D_f + P_b D_b \quad (15)$$

is the population-weighted average diffusion coefficient.

In the case of this simple two-site model as depicted in **Figure 2**, the bound population is given by

$$P_b = \alpha - \sqrt{\alpha^2 - \beta} \quad (16)$$

and

$$\alpha = \frac{\left(C_L + nC_P + K_d\right)}{2C_L} \text{ and } \beta = \frac{nC_P}{C_L} \quad (17)$$

where C_L and C_P are the total concentrations of ligand and protein, respectively. D_f can be determined by measuring the diffusion of the ligand in protein free solution, and D_b can normally be taken as equal to the protein diffusion coefficient since the binding of the ligand should have negligible effect on the diffusion coefficient of the (much larger) protein molecule.

5. Solution Dynamics and Organization Studied by PGSE NMR Diffusion Measurements

Supercooled Water

The anomalous behaviour of supercooled water is not only poorly understood, but it is also difficult to study due to it being in a metastable state [39]. The nature of the water to ice transition is of particular interest and many theoretical models have been proposed to understand it. The decrease in motion and increase in ordering will be reflected as changes in the translational motion of the water molecules. Such data also allows theoretical models of water to be more stringently tested. The results of diffusion measurements of supercooled water down to 238 K [1] and heavy water down to 244 K [40] are presented in Figure 3. Such data is often analysed by using the empirical Vogel-Tamman-Fulcher (VTF)-type relationship,

$$D = D_0 \exp\left(\frac{-B}{T - T_0}\right) \tag{18}$$

where T_0, D_0 and B are fitting constants; or the fractional power law (FPL),

$$D = D_0 T^{1/2}\left(\frac{T}{T_S} - 1\right)^{\gamma} \tag{19}$$

where γ (not the gyromagnetic ratio) is a fitting parameter and T_S represents a low temperature limit where D extrapolates to zero. A good fit to the FPL equation would imply that there was no continuity between states. At lower temperatures the FPL equation provides a slightly better fit to the data.

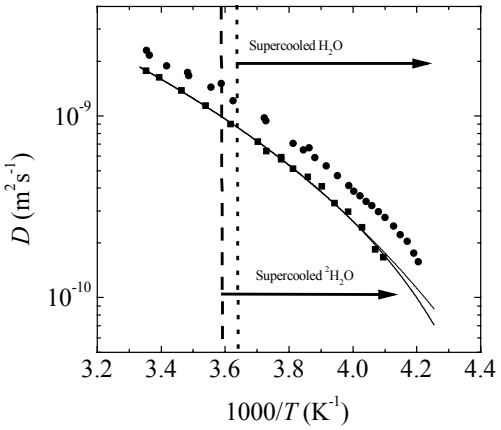

Figure 3. An Arrhenius plot of the diffusion coefficients of ^2H_2O (■) and ^1H_2O (●). The results of regressing the VTF (—) and FPL equation (- - -) onto the ^2H_2O data is also shown. The parameters for ^1H_2O are $D_0 = 4.00 \pm 0.87 \times 10^{-8}$ m^2s^{-1}, $B = 371 \pm 45$ K and $T_0 = 169.7 \pm 6.1$ K for the VTF equation and $D_0 = 7.66 \pm 0.24 \times 10^{-10}$ m^2s^{-1}, $T_S = 219.2 \pm 2.6$ K and $\gamma = 1.74 \pm 0.10$ for the FPL equation. Modified from ref. [40].

Alcohol-Water

A significant advantage of PGSE NMR over other techniques for measuring diffusion is its capability of determining the diffusion behaviour of many of the species in a solution simultaneously. The diffusion coefficient of all species in an ethanol-water solution are presented in Figure 4 and the Stokes radii of the ethanol and water calculated from this diffusion data are given in Figure 5. Such detailed data shows that ethanol can strongly interact with water through hydrogen bonding and implies that there is significant alcohol self-association at low ethanol mole fractions [41]. As expected from the Stokes-Einstein equation (Eq. (2)) the maximum in viscosity coincides with the diffusion minima.

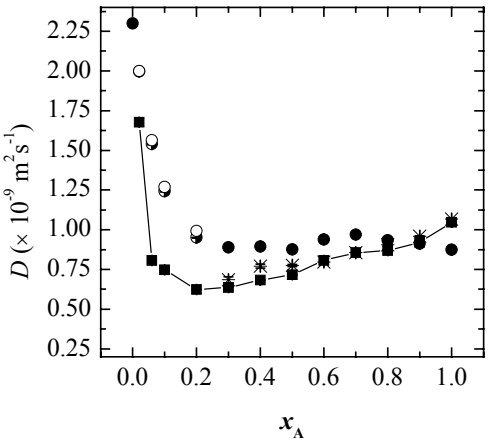

Figure 4. Diffusion coefficients of the alkyl (■), hydroxyl (✳), water (●) and water-hydroxyl (◑) groups at 298 K at various ethanol mole fractions, x_A, in the ethanol-water system. Modified from ref. [41]

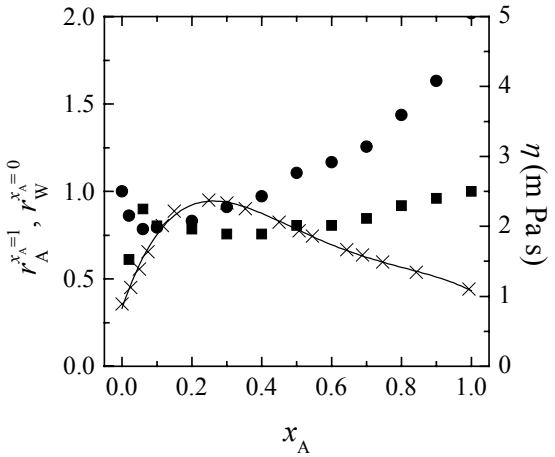

Figure 5. The effective radii of the ethanol (r_A, ■) and water (r_W, ●) determined from the ethanol and water diffusion coefficients and literature values of the solution viscosities [42] at 298 K using Eq. (2) for the ethanol-water system. Values of the solution viscosity at the same x_A used in the present work were determined by interpolation of the viscosity data (×) with a 5th order polynomial (—). The effective radii are normalized according to the respective pure solvent values.

‘Isolated’ Water Molecules

The unusual physical properties of water largely results from long-ranged structural correlations in the random and transiently hydrogen-bonded network that develops at low temperatures [43]. It is thus interesting to study the behaviour of isolated water molecules in a hydrophobic solvent. In **Figure 6** the temperature dependence of the translational and reorientational behaviour of (^{17}O-labelled) water measured using ^{17}O NMR (determined using PGSE NMR and longitudinal relaxation time measurements, respectively) are contrasted with the diffusion of nitromethane in a mixture of these two components. The results for the water are, not surprisingly, quite different from that for bulk water.

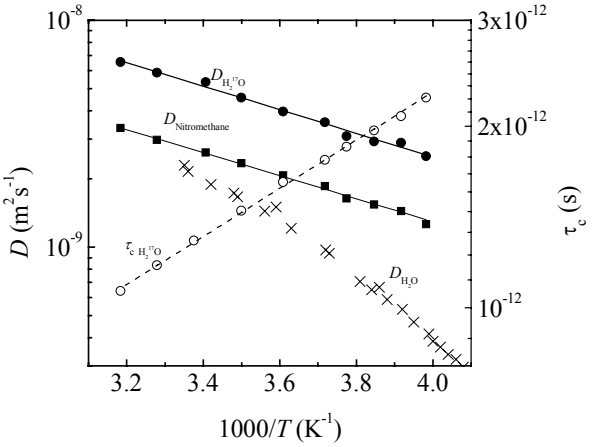

Figure 6. A plot of the $H_2{}^{17}O$ (●) and nitromethane (■) diffusion coefficients and $H_2{}^{17}O$ correlation time, τ_c (○), versus temperature in the nitromethane $H_2{}^{17}O$ mixture. The temperature dependence of the data sets were well described by an Arrhenius function (lines). From the data the activation energy for the reorientational motion was determined to be 7.7 ± 0.1 kJ mol^{-1}, similarly the activation energies for $H_2{}^{17}O$ and nitromethane diffusion were found to be 10.0 ± 0.3 kJ mol^{-1} and 9.7 ± 0.2 kJ mol^{-1}, respectively. For comparison, the diffusion data for pure H_2O (×) is also included. Modified from refs. [1,44].

Surfactants

Diffusion measurements have found a great deal of application in the study of surfactants due to their sensitivity to molecular organization and consequently for determining parameters such as the critical micellar concentration (cmc). An associating surfactant system is typically modelled using a two-site exchange model. In this case,

and assuming fast exchange the observed diffusion coefficient is expressed as a population weighted average between “free” and “bound” (i.e. surfactants in micelles) surfactant (i.e., see Eq. (15)) [13]. An example of determining the cmc from diffusion data is given in Figure 7.

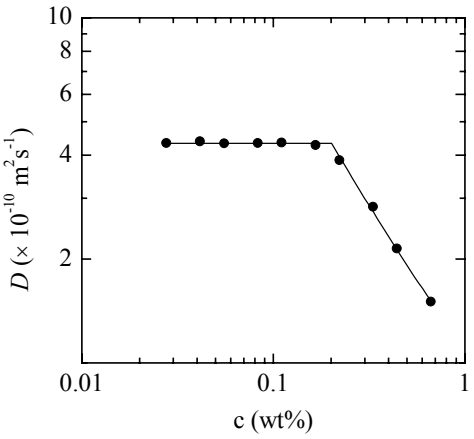

Figure 7. Determination of the cmc of sodium dodecyl sulfate (SDS) in D_2O from NMR diffusion measurements as a function of surfactant concentration (c). The break in the data at c = 0.2wt% represents the cmc. Modified from ref. [45].

Ionic Liquids

Room-temperature ionic liquids (RTIL), i.e., room-temperature molten salts, are non-flammable, have negligible vapor pressure and high ionic conductivity and are currently of great interest due to their potential application to devices such as solar cells, fuel cells, double-layer capacitors, and batteries. However, the ion net mobility and the ionic conduction mechanisms are not well understood, because the electrolytes are composed completely of ions without any neutral organic solvents. PGSE NMR has an important role to play in clarifying such mechanisms, especially since it allows the translational motion of all of the species present to be studied. In Figure 8 the temperature dependence of the self-diffusion of the components of an RTIL (1-ethyl-3-methyl-imidazolium tetrafluoroborate; [emim][BF_4]) including a lithium salt ($LiBF_4$) are presented. The results show that [emim] diffuses slightly faster than BF_4 even though the molecular size of [emim] is slightly larger than that of BF_4; this implies that BF_4 does not diffuse as a single ion [46].

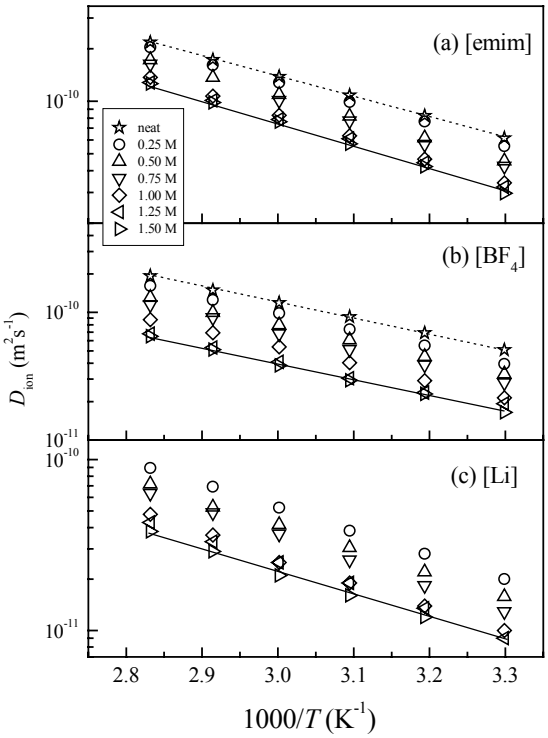

Figure 8. Arrhenius plots of the self-diffusion coefficients for (a) [emim], (b) BF_4 and (c) Li. The salt concentrations are noted in the figure. Modified from [46].

Drug Binding

In the simplest case, performing a single diffusion measurement of a ligand (e.g., a drug molecule) in the presence of a protein can provide information as to whether the drug binds to the protein. However, by performing a series of measurements with various ligand concentrations it is possible to determine the binding constant. An example of an NMR diffusometry study of a drug, salicylate, binding to the protein, serum albumin, is given in Figure 9 and analysis of the data from a series of such experiments using the two-site binding model (Eqs. (15)-(17)) is given in Figure 10. The poor fit to the entire data set indicates that the model is too simplistic and/or the assumptions inherent in the model are not met. At the highest drug concentration it is likely that there is self-association of both the drug and the albumin.

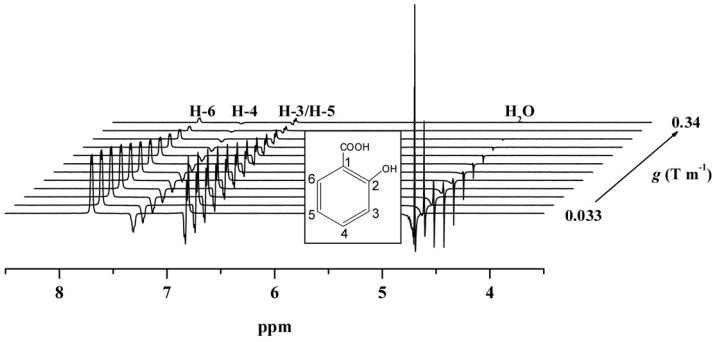

Figure 9. 500 MHz ^{1}H PGSE spectra of 80 mM salicylate and 0.5 mM bovine serum albumin in water at 298 K. The spectra were acquired using the Hahn spin-echo based PGSE-WATERGATE sequence in which the usual π rf pulse is replaced by a binomial π pulse as in a WATERGATE sequence to provide solvent suppression. The (residual) water resonance gives rise to the peak at 4.7 ppm and the three peaks to the left originate from salicylate (from left to right: H-6, H-4, H-3/H-5; also see inset). Modified from ref. [47].

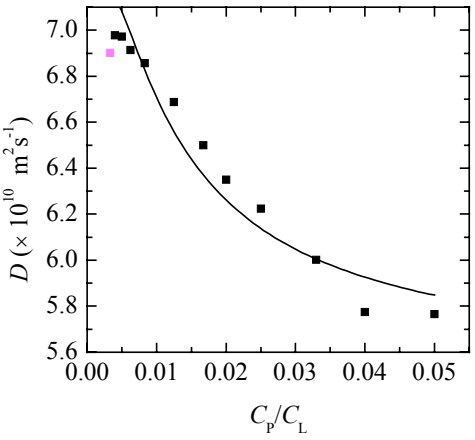

Figure 10. Diffusion of salicylate in 0.5 mM bovine serum albumin measured using ^{1}H PGSE NMR at 500 MHz. The errors in each measurement are typically less than 1%. The curve is the result of regressing the two-site model (i.e., Eq. (15)) onto the data (excluding the highest salicylate concentration) giving $K_d = 0.030 \pm 0.004$ M with $n = 33 \pm 3$. Modified from ref. [47].

Protein Association

Protein association phenomena are necessary steps in pharmacology, protein aggregation and crystallisation [48-51]. Except at very low concentrations, many proteins are in some equilibrium between different aggregation states (e.g., monomer ↔ higher oligomer). The 'environment' (e.g., macromolecular crowding, hydration, counterions, pH, temperature) around the protein molecules modulates the interactions (e.g., electrostatic [52-55] and hydrophobic hydration [41]) that control association. But despite a long history of study, the extent, kinetics and mechanisms remain poorly understood (e.g., see ref. [56]), and generally only empirical rules exist on the choice of solvent, pH, ionic concentration and choice of salt (e.g., the Hofmeister series) in explaining how to modulate biomolecular association [57]. In Figure 11 the change in the average molecular weight with time of lysozyme oligomers *still in solution* (NB as the lysozyme oligomers increase in size they gradually become NMR invisible due to shortening spin-spin relaxation times) in aggregating lysozyme solutions is presented for four initial lysozyme monomer concentrations. Because the measurements were conducted at reasonably high protein concentrations, self-obstruction (i.e., 'crowding') effects can be expected. Hence, the diffusion coefficients are not only reduced on account of monomers associating to form higher oligomers but also because of obstruction. Thus the PGSE experiment gives weighted average diffusion coefficient including the effects of crowding, $\langle D \rangle^C$. The diffusion data was obtained from PGSE NMR diffusion measurements and then recast in terms of the average molecular weight $\langle Mw \rangle^C$ using the Stokes-Einstein equation (Eq. (2)). This data provides a means for understanding the crystal sizes that result from different initial protein concentrations [58].

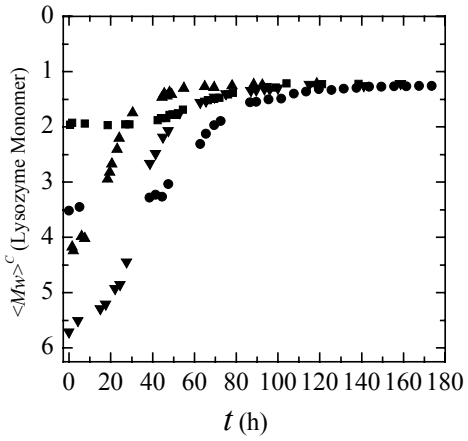

Figure 11. The time dependence of the average molecular weight including the effects of crowding, $\langle Mw \rangle^C$ determined from PGSE NMR measurements of four different lysozyme samples with different initial (i.e., monomer) concentrations (3 mM, ■; 5 mM, ●; 6 mM, ▲; 7 mM, ▼) at pH 6 and 298 K in 0.5 M NaCl. At long times the values plateau out to a value just slightly greater than that expected for a monomer. Modified from ref. [58].

6. Acknowledgement

The NSW State Government is acknowledged for support through a BioFirst award.

7. References

[1] W.S. Price, H. Ide, and Y. Arata, J. Phys. Chem. A 103 (1999) 448-450.
[2] W.S. Price, N.-H. Ge, and L.-P. Hwang, J. Magn. Reson. 98 (1992) 134-141.
[3] P.T. Callaghan, Aust. J. Phys. 37 (1984) 359-387.
[4] P. Stilbs, Prog. NMR Spectrosc. 19 (1987) 1-45.
[5] J. Kärger, H. Pfeifer, and W. Heink, Adv. Magn. Reson. 12 (1988) 1-89.
[6] P.T.Callaghan, Principles of Nuclear Magnetic Resonance Microscopy, Clarendon Press**,** Oxford. 1991.
[7] W.S. Price, in: G.A. Webb (Ed.), Annual Reports on NMR Spectroscopy, Academic Press, London. 1996. p. 51-142

[8] R.Kimmich, NMR: Tomography, Diffusometry, Relaxometry, Springer Verlag, Berlin. 1997.
[9] C.S. Johnson, Jr., Prog. NMR Spectrosc. 34 (1999) 203-256.
[10] P. Stilbs, in: J.C. Lindon, G.E. Tranter, J.L. Holmes (Eds.), Encyclopedia of Spectroscopy and Spectrometry, Academic Press, London. 2000. p. 369-375
[11] S. Matsukawa, H. Yasunaga, C. Zhao, S. Kuroki, H. Kurosu, and I. Ando, Progress in Polymer Science 24 (1999) 995-1044.
[12] W.S. Price, in: G.A. Webb (Ed.), Annual Reports on the Progress in Chemistry Section C, Royal Society of Chemistry, London. 2000. p. 3-53
[13] O. Söderman and P. Stilbs, Prog. NMR Spectrosc. 26 (1994) 445-482.
[14] I. Furó, J. Mol. Liquids 117 (2005) 117-137.
[15] M. Lin, M.J. Shapiro, and J.R. Wareing, J. Org. Chem. 62 (1997) 8930-8931.
[16] A.R. Waldeck, P.W. Kuchel, A.J. Lennon, and B.E. Chapman, Prog. NMR Spectrosc. 30 (1997) 39-68.
[17] L. Fielding, Tetrahedron 56 (2000) 6151-6170.
[18] W.S. Price, in: D.M. Grant, R.K. Harris (Eds.), Encyclopedia of Nuclear Magnetic Resonance, Wiley, New York. 2002. p. 364-374
[19] J.Crank, The Mathematics of Diffusion, Oxford University Press, Oxford. 1975.
[20] M.A.Lauffer, Motion in Biological Systems, Alan R. Liss, Inc., New York. 1989.
[21] E.L.Cussler, Diffusion Mass Transfer in Fluid Systems, Cambridge University Press, Cambridge. 1997.
[22] H.J.V.Tyrrell and K.R.Harris, Diffusion in Liquids: A Theoretical and Experimental Study, Butterworths, London. 1984.
[23] A.M. Berezhkovskii and G. Sutmann, Phys. Rev. E 65 (2002) 060201-1-060201-4.
[24] A.Einstein, Investigations on the Theory of Brownian Movement, Dover, New York. 1956.
[25] B.E.Poling, J.M.Prausnitz, and J.P.O'Connell, The Properties of Gases and Liquids, McGraw Hill, New York. 2001.
[26] E.O. Stejskal and J.E. Tanner, J. Chem. Phys. 42 (1965) 288-292.
[27] J.E. Tanner, J. Chem. Phys. 52 (1970) 2523-2526.
[28] W.S. Price, P. Stilbs, B. Jönsson, and O. Söderman, J. Magn. Reson. 150 (2001) 49-56.
[29] W.S. Price, K. Hayamizu, H. Ide, and Y. Arata, J. Magn. Reson. 139 (1999) 205-212.
[30] N. Hedin and I. Furó, J. Magn. Reson. 131 (1998) 126-130.
[31] N. Hedin, T.Y. Yu, and I. Furó, Langmuir 16 (2000) 7548-7550.
[32] W.S. Price and M. Wälchli, Magn. Reson. Chem. 40 (2002) S128-S132.
[33] W.S. Price and O. Söderman, Israel. J. Chem. 43 (2003) 25-32.
[34] J.E. Tanner and E.O. Stejskal, J. Chem. Phys. 49 (1968) 1768-1777.
[35] J. Kärger and W. Heink, J. Magn. Reson. 51 (1983) 1-7.
[36] D.G.Duffy, Green's Functions with Applications, CRC, Boca Raton. 2001.
[37] H.C. Torrey, Phys. Rev. 104 (1956) 563-565.
[38] W.S. Price, Concepts Magn. Reson. 9 (1997) 299-336.

[39] C.A. Angell, in: F. Franks (Ed.), Water and Aqueous Solutions at Subzero Temperatures, Plenum, New York. 1982. p. 1-81
[40] W.S. Price, H. Ide, Y. Arata, and O. Söderman, J. Phys. Chem. B 104 (2000) 5874-5876.
[41] W.S. Price, H. Ide, and Y. Arata, J. Phys. Chem. A 107 (2003) 4784-4789.
[42] K.R. Harris and H.N. Lam, J. Chem. Soc. , Faraday Trans. 91 (1995) 4071-4077.
[43] F.X. Prielmeier, E.W. Lang, R.J. Speedy, and H.-D. Lüdemann, Ber. Bunsenges. Phys. Chem. 92 (1988) 1111-1117.
[44] W.S. Price, H. Ide, and Y. Arata, J. Chem. Phys. 113 (2000) 3686-3689.
[45] E. Pettersson, D. Topgaard, P. Stilbs, and O. Söderman, Langmuir 20 (2004) 1138-1143.
[46] K. Hayamizu, Y. Aihara, H. Nakagawa, T. Nukuda, and W.S. Price, J. Phys. Chem. B 108 (2004) 19527-19532.
[47] W.S. Price, F. Elwinger, C. Vigouroux, and P. Stilbs, Magn. Reson. Chem. 40 (2002) 391-395.
[48] L.R. De Young, A.L. Fink, and K.A. Dill, Acc. Chem. Res. 26 (1993) 614-620.
[49] A.McPherson, Crystallization of Biological Macromolecules, Cold Spring Harbor Laboratory Press**,** New York. 1999.
[50] R. Piazza, Current Opinion in Colloid & Interface Science 5 (2000) 38-43.
[51] W.S. Price, Aust. J. Chem. 56 (2003) 855-860.
[52] P.Turq, J.Barthel, and M.Chemla, Transport, Relaxation and Kinetic Processes in Electrolyte Solutions, Springer-Verlag**,** Berlin. 1992.
[53] B.H. Honig and A. Nicholls, Science 268 (1995) 1144-1149.
[54] J.W. Pitera, M. Falta, and W.F. van Gunsteren, Biophys. J. 80 (2001) 2546-2555.
[55] P. Vagedes, W. Saenger, and E.-W. Knapp, Biophys. J. 83 (2002) 3066-3078.
[56] M.M. Crnogorac, G.M. Ullmann, and N.M. Kostic, J. Am. Chem. Soc. 123 (2001) 10789-10798.
[57] S.N. Timasheff, Annu. Rev. Biophys. Biomol. Struct. 22 (1993) 67-97.
[58] W.S. Price, F. Tsuchiya, and Y. Arata, Biophys. J. 80 (2001) 1585-1590.